A Study of Drag Force in Isothermal Bubbly Flow

C. Li[1], S.C.P. Cheung[1], G.H. Yeoh[2,3] and Tu, J.Y.[1]
[1]School of Aerospace, Mechanical and Manufacturing Engineering,
RMIT University, Victoria 3083, Australia
e-mail: jiyuan.tu@rmit.edu.au
[2]Australian Nuclear Science and Technology Organisation (ANSTO),
PMB 1, Menai, NSW 2234, Australia
[3]School of Mechanical and Manufacturing Engineering,
University of New South Wales, Sydny 2052, Australia

Received: 3rd September 2009, Accepted: 2nd November 2009

Abstract
Driven by the extensive demands of simulating highly concentrated gas bubbly flows in many engineering fields, numerical studies have been performed to investigate the neighbouring effect of a swarm of bubbles on the interfacial drag forces. In this study, a novel drag coefficient correlation (Simonnet et al., 2007) in terms of local void fraction coupled with the population balance model based on average bubble number density (ABND) has been implemented and compared with Ishii-Zuber densely distributed fluid particles drag model. The predicted local radial distributions of three primitive variables: gas void fraction, Sauter mean bubble diameter, and gas velocity, are validated against the experimental data of Hibiki et al. (2001). In general, satisfactory agreements between predicted and measured results are achieved by both drag force models. With additional consideration for closely packed bubbles, the latest coefficient model by Simonnet et al. (2007) shows considerably better performance in capturing the reduction of drag forces incurred by neighbouring bubbles.

Keywords: Multi-phase flow; Transition regime; Drag coefficient; Local void fraction; Population balance approach; ABND model

NOMENCLATURE

a_{if}	Interfacial area concentration
C_D	Drag coefficient
$C_{D\infty}$	Drag coefficient of isolated bubble in an infinite medium
C_L	Lift coefficient
d_H	Maximum bubble horizontal dimension
D	Inner diameter of the pipe
D_s	Bubble Sauter mean diameter
E_o	Eötvos number
F_i	Total interfacial force
$F_{\text{lg}}^{\text{drag}}$	Drag force
$F_{\text{lg}}^{\text{lift}}$	Lift force
$F_{\text{lg}}^{\text{lubrication}}$	Wall lubrication force
$F_{\text{lg}}^{\text{dispersion}}$	Turbulent dispersion force
IAC	Interfacial area concentration
g	Gravitational acceleration
$\vec{g}$	Gravitational vector
k	Turbulent kinetic energy
$\vec{n}_w$	Outward vector normal to the wall surface
n	Average number density of gas phase (bubble)

P	Pressure
Re	Flow Reynolds number
Re_m	Mixture Reynolds number
u_∞	Velocity of an isolated bubble in a quiescent liquid
u	Velocity
$\vec{u}$	Velocity vector
We	Weber number
We_{cr}	Critical Weber number
y_w	Adjacent point normal to the wall surface

Greek Symbols

α	Void fraction
α_{gm}	Maximum packing value
α_{max}	Maximum allowable void fraction
α_{loc}	Local void fraction
ε	Turbulence kinetic energy dissipation
μ^e	Effective viscosity
μ_m	Mixture viscosity
$v_{t,g}$	Turbulent kinematic viscosity
ρ	Density
$\Delta\rho$	Density difference = $\rho_l - \rho_g$
σ	Surface tension
ϕ_n^{RC}	Bubble number density change rate due to random collision
ϕ_n^{TI}	Bubble number density changes rate due to impact of turbulent eddies
ϕ_n^{WE}	Bubble number density changes rate due to wake entrainment

Subscripts

g	Gas
gl	Transfer of quantities from liquid phase to vapour phase
i	Index of gas/liquid phase
l	Liquid
lg	Transfer of quantities from gas phase to liquid phase

1. INTRODUCTION

Two-fluid model based on the inter-penetrating continua approach is probably considered to be the most detailed and accurate macroscopic formulation of gas-liquid flow systems. Herein, exchanges that occur at the interface between the two phases are explicitly accounted and the dynamics of the interaction are fully described through appropriate constitutive relations governing the inter-phase mass, momentum and energy exchanges. The existence of these terms is one of the most important characteristics of the two-fluid model formulation since they determine not only the degree of mechanical and thermal non-equilibrium but also the rate of phase changes between phases.

In the absence of heat and mass transfer, the complexity of the problem reduces to consideration of only the momentum exchange term, which is typical of isothermal bubbly flow. The interfacial transfer in the conservation momentum equation generally involves the consideration of drag and non-drag interfacial force densities. The interfacial drag force is a result of the shear and form drag of the fluid flow, which depends on the drag coefficient as well as the interfacial area concentration. For solid particles, the drag coefficient depends only on the characteristics of the flow surrounding the particle and is primarily a function of the particle Reynolds number and of the turbulence intensity of the continuous phase (Bertola et al. 2004). For bubbles, the behaviours are however complicated due to three important aspects. Firstly, when the liquid is pure enough, it has the possibility to slip along the surface of the bubbles. This is in contrast to flow past rigid (solid) bodies where the no-slip condition is imposed. Secondly, almost all the inertia is contained in the liquid due to the relative weak density of bubbles compared to that of the liquid; thus inertia induced hydrodynamic forces is particularly important in the prediction of bubble motion. Thirdly, bubbles have a tendency to deform due to coalescence and break-up; the changes of bubble shape add new degrees of freedom to an already complex problem (Magnaudet and Eames 2000).

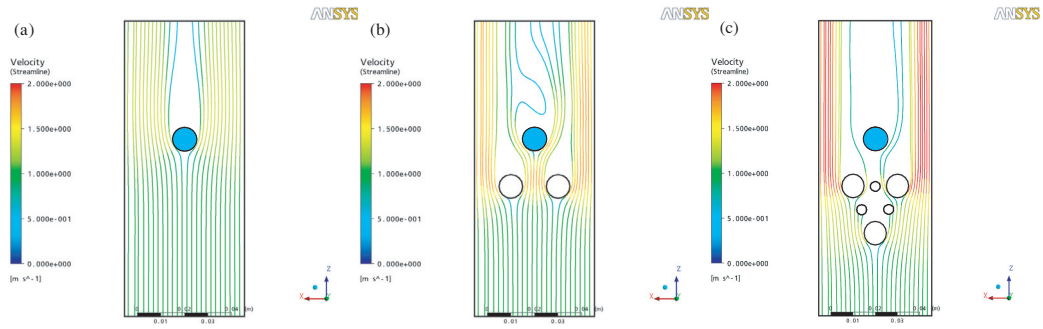

Case A Case B Case C

CASE	*Drag Force for Monitored Bubble [N]*	*Drag Coefficient for Monitored Bubble [-]*
A	0.000 436	0.011 121
B	0.000 641	0.016 356
C	0.000 252	0.006 434

- presents the monitored bubble
- The liquid is water with 1 m/s uniform inlet velocity for all cases.

Figure 1. Streamline of liquid velocity passing through single bubble and multi-bubbles.

The mutual interaction among bubbles can also have a significant influence on the drag force (Behzadi et al. 2004; Bertola et al. 2004; and Simonnet et al. 2007). Figure 1 illustrates the velocity streamline of liquid passing through the cases of single bubble and multi-bubbles with uniform incoming velocity. It demonstrates that the drag force of the monitored bubble has been significantly affected by its neighbouring bubbles. In Figure 1(b), after passing other two bubbles, the liquid velocity distributions are not uniform any more, presenting higher liquid velocity brushing monitored bubble. It leads to higher drag force comparing with single bubble case in Figure 1(a). However, the drag force for case C is comparatively lower than single bubble case since the observed bubble is under the wake area of front bubbles.

Over the years, several models have been proposed to calculate the drag force for bubbles at high void fractions. Ishii and Zuber (1979) have categorized the bubbly flow behaviours into different regimes. A mixture viscosity model has been developed to obtain each drag coefficient correlations for the individual flow regimes. CFX commercial software drag coefficient model based on Ishii and Zuber (1979)'s drag formulations has been widely applied and can yield reasonable predictions for a range of flow conditions. Many recent investigations by Rusche and Issa (2000), Behzadi et al. (2004) and Simonnet et al. (2007) have nevertheless focused on the modelling of suitable drag coefficient multiplier across a wide range of void fractions and different flow regimes. Through this approach, the ratio of the drag coefficient to its single dispersed element value can be fitted to a function of the phase fraction, i.e. $C_D/C_{D\infty} = f(\alpha)$ where $C_{D\infty}$ is the drag coefficient of an isolated bubble in an infinite medium. Simonnet et al. (2007) have developed a novel drag coefficient expression by correlating the drag coefficient multiplier with exhaustive experimental data. The improved expression to predict two-phase flow from bubbly to slug transitional regime is investigated in the present study. Within this regime, bubbles are generally found to be highly distorted and closely packed in contrast to the bubbly flow regime of which the bubbles are normally spherical in shape and allowed to move freely (Hibiki et al., 2001 and Cheung et al., 2007).

The primary aim of this paper is to compare the relative merits and capabilities applying two drag coefficient formulations commonly used Ishii and Zuber (1979) model and recently proposed by Simonnet et al. (2007) to evaluate the drag force in the conservation momentum equation. In order to predict the dynamic changes of the interfacial structure, the use of first-order equation to characterise the transport of interfacial area concentration (Hibiki and Ishii, 2002, Yao and Morel, 2004) or averaged bubble number density (ABND) (Cheung et al. 2007) has sufficed. The ABND model (Cheung et al. 2007) is thus employed to predict the local bubble distribution in an upward flow channel and special emphasis is directed towards investigations on bubbly-to-slug transitional regime (cap-bubbly flow condition) where high void fraction and high liquid velocity exist. Numerical predictions through these two drag coefficient correlations are compared against experimental data of isothermal gas-liquid bubbly flow in a vertical pipe performed by Hibiki et al. (2001).

2. MATHEMATICAL MODELS

2.1 Two-Fluid and ABND models

The two-fluid model conservation equations for mass and momentum for bubbly flows can be written as:

$$\frac{\partial\left(\rho_i\alpha_i\right)}{\partial t}+\nabla\cdot\left(\rho_i\alpha_i\vec{u}_i\right)=0 \tag{1}$$

$$\frac{\partial\left(\rho_i\alpha_i\vec{u}_i\right)}{\partial t}+\nabla\cdot\left(\rho_i\alpha_i\vec{u}_i\vec{u}_i\right)=-\alpha_i\nabla P+\alpha_i\rho_i\vec{g}+\nabla\cdot\left[\alpha_i\mu_i^e\left(\nabla\vec{u}_i+\left(\nabla\vec{u}_i\right)^T\right)\right]+F_i^D+F_i^{ND} \tag{2}$$

where F_i^D is the interfacial drag force density while F_i^{ND} consists of the non-drag force contributions.

For dispersed isothermal bubbly flow, the average bubble number density transport equation takes the form:

$$\frac{\partial n}{\partial t}+\nabla\cdot\left(\vec{u}_g n\right)=\phi_n^{RC}+\phi_n^{TI}+\phi_n^{WE} \tag{3}$$

where n is the average bubble number density and $\vec{u}_g$ is the mean gas velocity. The phenomenological mechanisms of coalescence and breakage are effected through the source and sink terms ϕ_n^{RC}, ϕ_n^{TI} and ϕ_n^{WE} of which they are due to random collision, turbulent induced breakage and wake entrainment. The Yao and Morel (2004) model is adopted in the present study. According to the research of Hibiki and Ishii (2000), it was found that wake entrainment phenomenon only play significant influence in slug flow. Therefore, in this study, wake entrainment has been ignored. More details regarding the model can be referred in Cheung et al. (2007a, 2007b).

2.2 Interfacial Momentum Transfer due to Drag

The inter-phase momentum transfer between gas and liquid due to the drag force resulted from shear and form drag and can be modelled in terms of the interfacial area concentration a_{if} and slip velocity $\left(\vec{u}_g-\vec{u}_l\right)$ as:

$$F_{l\to g}^{\mathrm{D}}=-F_{g\to l}^{\mathrm{D}}=\frac{1}{8}C_D a_{if}\rho_l\left|\vec{u}_g-\vec{u}_l\right|\left(\vec{u}_g-\vec{u}_l\right) \tag{4}$$

It should be noted that $F_{l\to g}$ in the above equation depicts the momentum transfer from the gas phase to the liquid phase and vice versa for $F_{g\to l}$. In the present study, two correlations of several distinct Reynolds number regions for individual bubbles proposed by Ishii and Zuber (1979) and Simonnet el al. (2007) are employed to evaluate the drag coefficient C_D in equation (4).

Ishii and Zuber (1979) drag coefficient correlation takes into account for multi-bubble effects by considering different bubble shape regimes; such as: dense spherical particle regime, dense distorted particle regime and dense spherical cap regime.

Dense Spherical Particle Regime

$$C_D(sphere)=\frac{24}{Re_m}(1+0.15Re_m^{0.687}) \tag{5}$$

Dense Distorted Particle Regime

$$C_D(ellipse)=\frac{2}{3}\sqrt{Eo}E \tag{6}$$

Dense Spherical Cap Regime

$$C_D(cap)=\frac{8}{3}E' \tag{7}$$

From above, the mixture Reynolds number Re_m is given by in terms of the Sauter bubble diameter D_s as

$$Re_m=\frac{\rho_l\left|u_g-u_l\right|D_s}{\mu_m} \tag{8}$$

where, the mixture viscosity μ_m can be evaluated according to

$$\frac{\mu_m}{\mu_l} = (1 - \frac{\alpha_g}{\alpha_{gm}})^{-2.5\alpha_{gm}\frac{\mu_g + 0.4\mu_l}{\mu_g + \mu_l}} \quad (9)$$

In equation (6), the dense distorted particle regime drag coefficient model takes the form of a multiplying factor E, which is given in terms of the void fraction as

$$E = \left[\frac{1 + 17.67 f(\alpha_g)^{6/7}}{18.67 f(\alpha_g)}\right]^2 \quad (10)$$

Where

$$f(\alpha_g) = \frac{\mu_l}{\mu_m}(1 - \alpha_g)^{1/2} \quad (11)$$

And, Eo represents the Eotvos number which is defined by

$$Eo = \frac{g\left(\rho_l - \rho_g\right)D_s^2}{\sigma} \quad (12)$$

where σ is the surface tension coefficient.

For dense spherical cap regime, the multiplication factor E' takes however the form:

$$E' = (1 - \alpha_g)^2 \quad (13)$$

As implemented within ANSYS CFX 11 (ANSYS, 2005. CFX-11 User Manual) the regime selection is based on

$$C_D = \begin{cases} C_D(sphere) & if C_D(sphere) \geq C_D(ellipse) \\ \min(C_D(ellipse), C_D(cap)) & if C_D(sphere) \leq C_D(ellipse) \end{cases} \quad (14)$$

On the other hand, through recent experimental investigation by Simonnet et al. (2007), a novel drag correlation for pure air-water systems has been proposed. It can be written as

$$C_D = C_{D\infty}E'' \quad (15)$$

where $C_{D\infty}$ is the drag coefficient of an isolated bubble in an infinite medium, which can be obtained through the balance of buoyancy, drag and gravitational as

$$C_{D\infty} = \frac{4}{3}\frac{\rho_l - \rho_g}{\rho_l} g D_s \frac{1}{u_\infty^2} \quad (16)$$

In the above equation, u_∞ represents the velocity of an isolated bubble in a quiescent liquid which can be calculated using the correlation of Jamialahmadi et al. (1994):

$$u_\infty = \frac{u_{b1}u_{b2}}{\sqrt{u_{b1}^2 + u_{b2}^2}} \quad (17)$$

where

$$u_{b1} = \frac{1}{18}\frac{\rho_l - \rho_g}{\mu_l} g D_s^2 \frac{3\mu_g + 3\mu_l}{3\mu_g + 2\mu_l} \quad (18)$$

$$u_{b2} = \sqrt{\frac{2\sigma}{D_s(\rho_l - \rho_g)} + \frac{gD_s}{2}} \quad (19)$$

In equation (16), the multiplication factor E'' according to Simonnet et al. (2007) is

$$E'' = (1-\alpha_g)[(1-\alpha_g)^m + (4.8\frac{\alpha_g}{1-\alpha_g})^m]^{-2/m} \tag{20}$$

Where, m is set a value of 25. The above modification is valid for a wide range of void fractions and across different flow regimes.

2.3 Interfacial Momentum Transfer due to Non-Drag Forces

Alongside with the drag force, other interfacial non-drag forces considered in the present study can be categorized into:

$$F_{l\to g}^{ND} = F_{l\to g}^{\text{lift}} + F_{l\to g}^{\text{wall lubrication}} + F_{l\to g}^{\text{turbulent dispersion}} \tag{21}$$

where the various forces in the above expression are due to lift, wall lubrication and turbulence dispersion. More details can be found in Cheung et al. (2007).

3. NUMERICAL DETAILS

The numerical model is validated against experiments conducted by Hibiki et al. (2001). Experiments for a range of superficial liquid velocities $\langle j_f \rangle$ and superficial gas velocities $\langle j_g \rangle$ at the location of z/D = 6.0 and 53.5 have been performed (see Figure 2a). Eight bubbly flow conditions, as summarized in Table 1, have been employed for validation. The eight flow conditions of Hibiki et al. (2001) have been depicted in Figure 3. Four conditions are in the bubbly flow and another four are in the bubbly-to-slug transitional regime, particularly cap bubbles were observed in flow condition of $\langle j_f \rangle$=0.986 m/s and $\langle j_g \rangle$=0.321 m/s. As demonstrated in Ho and Yeoh (2005), coalescence of capped bubbles and its interaction with bubbly flow mixtures may become significant in bubbly-to-slug transitional flow regime causing noticeable discrepancy between predicted results and measured data.

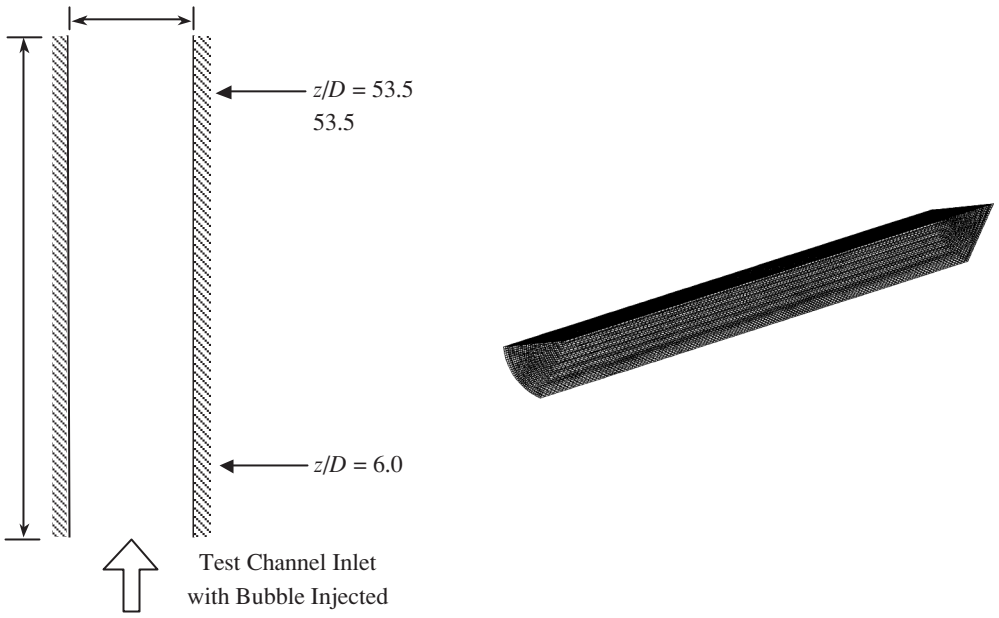

Figure 2. (a) Schematic drawing of the test section of Hibiki et al. (2001) experiment and (b) Visualization and mesh distribution of computational models: Hibiki et al. (2001)

Solutions to the two sets of balance equations for mass and momentum of each phase is sought. Radial symmetry has been assumed in which numerical simulations are performed on a 60 degree radial sector of the pipe with symmetry boundary conditions at both vertical sides. The computational mesh and geometry is shown in Figure. 2(b). At the inlet of the test section, as the

diameter of the injected bubbles are unknown, uniformly distributed superficial liquid and gas velocities, void fraction and bubble size are specified in accordance with the flow condition described. Details of the boundary conditions have been summarised in Table 1. The Shear Stress Transport (SST) turbulent model is employed in the present study. Moreover, to account for the effect of bubbles on liquid turbulence, the Sato's bubble-induced turbulent viscosity model (Sato et al., 1981) has been adopted.

Table 1. Bubbly flow conditions and its inlet boundary conditions employed in the present study

Superficial liquid velocity (m/s) $\langle j_f \rangle$	**Superficial gas velocity $\langle j_g \rangle$ (m/s)**			
	Hibiki et al. (2001) *experiment*			
0.491				
$[\alpha_g\|_{z/D=0.0}$ (%)]	0.0275	0.0556	0.129	0.190
$[D_S\|_{z/D=0.0}$ (mm)]	[5.0]	[10.0]	[20.0]	[25.0]
	[3.0]	[3.0]	[3.0]	[3.0]
0.986				
$[\alpha_g\|_{z/D=0.0}$ (%)]	0.0473	0.113	0.242	0.321[b]
$[D_S\|_{z/D=0.0}$ (mm)]	[5.0]	[10.0]	[20.0]	[25.0]
	[3.0]	[3.0]	[3.0]	[3.0]

[b] Cap bubbles were experimental observed in this flow condition.

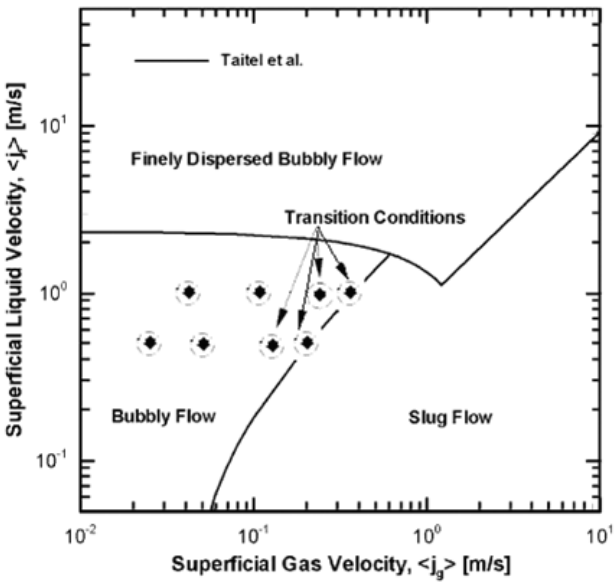

Figure 3. Map of tube flow regime and bubbly flow conditions studied in the present study

4. RESULT AND DISCUSSION

Intending to cover a wide range of flow conditions, eight different operations has been numerically implemented and validated against experimental data of Hibiki et al. (2001). By comparison of numerical results with experimental data for gas void fraction, Sauter mean bubble diameter and air velocity, values of the various adjustable parameters in the model are determined so as to give reasonable results over all operating conditions. Due to increased possibility of close package between bubbles under high void fraction flow condition, different breakage and coalescence calibration factors are applied for case of high void fraction (transitional flow) and comparatively low void fraction (bubbly flow). With higher void fraction (transitional flow), in the present study, the coalescence and breakage calibration factors are sent as 0.1 and 0.6 respectively. While 0.3 of

coalescence and 1 of breakage calibration factors are set for comparatively low void fraction (bubbly flow). The similar calibration factors adjustments were employed in research of Chen et al. (2005) and Olmos et al. (2001).

4.1 Void fraction distribution

The comparison between the experimental data of Hibiki et al. (2001) at the dimensionless axial position Z/D = 53.5 and predicted radial void fraction distributions using drag coefficient correlations of Simonnent et al. (2007) and Ishii and Zuber (1979) are depicted in Figure 4. In

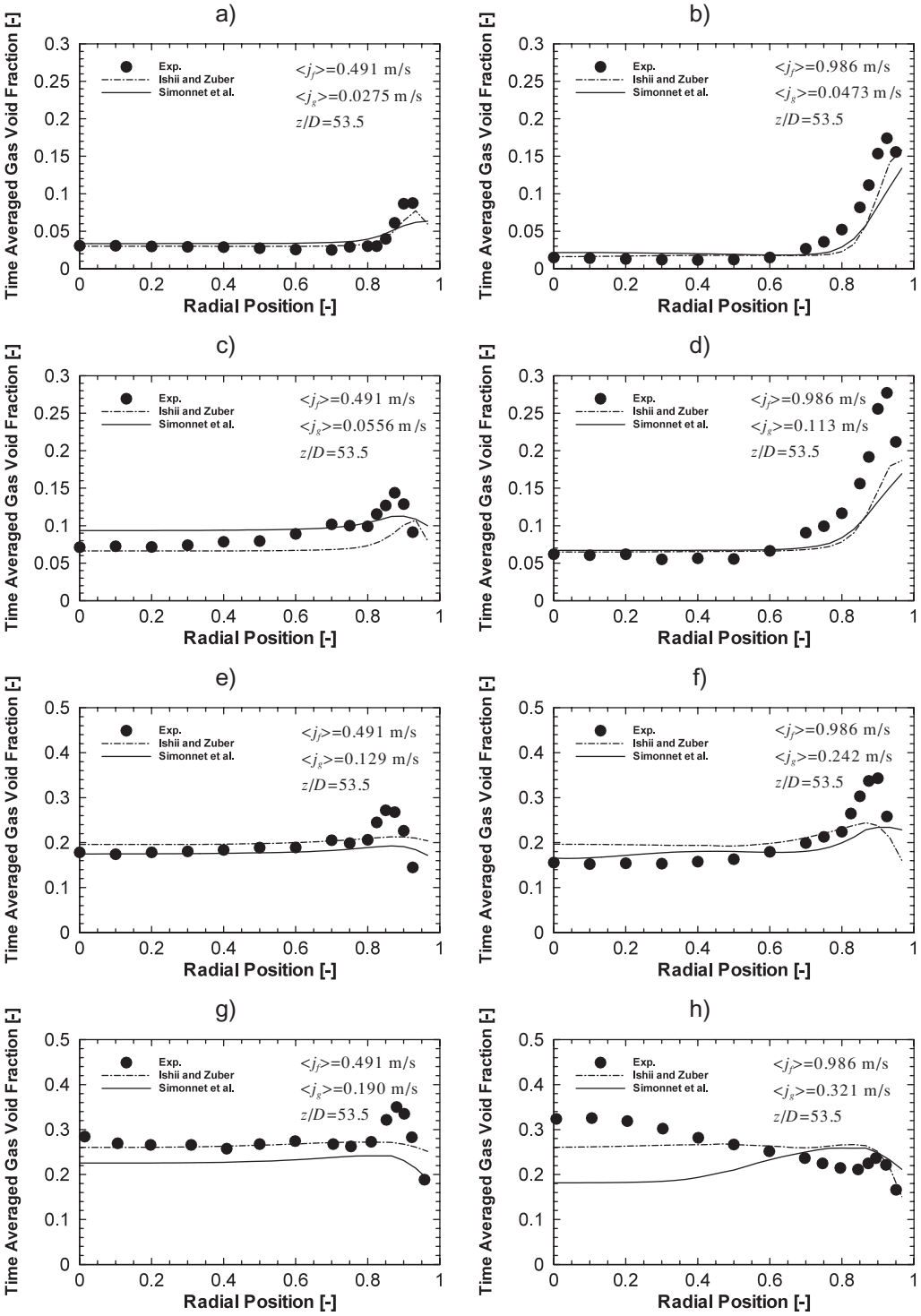

Figure 4. Predicted radial void fraction distributions and experiment data of Hibiki et al. (2001) at Z/D = 53.5.

isothermal gas-liquid bubbly flow, Hibiki et al. (2001) developed classification of phase distribution patterns into five basic types of distributions: "wall peak", "intermediate peak", "corn peak", "transition" and "flat". In the present research, the numerical research has been widely included "wall peak", "intermediate peak" and "transition". In general, both two drag coefficient correlation models give considerably reasonable good agreement with experimental results. For the flow condition of $\langle j_f \rangle$ =0.986 m/s and $\langle j_g \rangle$ =0.321 m/s, both two drag coefficient models perform considerably better prediction near the wall however void fraction at the core of pipe are under-predicted (Figure 4h). One of the possible reasons could be due to the lateral lift force which is the dominating factor for bubble migration between wall and pipe core. Tomiyama (1998) lift force correlation adopted in this study proposes that bubbles have the tendency to migrate toward the pipe centre to form "core peak" when bubbles diameters are larger than 5.8 mm for air-water bubbly upward system. However, according to experimental data of Hibiki et al. (2001), the gas void fraction distribution for flow condition of $\langle j_f \rangle$ =0.986 m/s and $\langle j_g \rangle$ =0.321 m/s shows "core peak" (see in figure 4h), even though the Sauter mean bubble diameters are less than 5.8mm (see in figure 5h). Another possible reason for discrepancies between the numerical and experimental results is due to Tomiyama (1998) lift force which conducted from single bubble behaviour in infinite stagnant liquid system. It might be a challenge to be adopted into swam bubbles flow condition at the current stage.

4.2 Sauter mean bubble diameter

Figure 5 illustrates the predicted and measured Sauter mean bubble diameter distributions, corresponding to that of void fraction profiles in Figure 4. Owing to the tendency of small bubbles migrating towards the wall, slightly larger bubbles are formed near the wall where highly concentred bubbles having greater possibility to colloid forming bigger bubbles. Therefore, the Sauter mean bubble diameter appeared almost uniform along the radial direction with slim larger value near the wall for most cases except for the flow condition of $\langle j_f \rangle$ =0.986 m/s and $\langle j_g \rangle$ =0.321 m/s. On the other hand, when the newly formed bubbles are big enough, they have the tendency to move towards to pipe centre and deform to cap bubbles. These cap bubbles have strong wake entrainment phenomenon, absorbing small bubbles in their wake area to form larger cap bubbles. According to the research of Hibiki et al. (2001), cap bubbles were observed at flow condition of $\langle j_f \rangle$ =0.986 m/s and $\langle j_g \rangle$ =0.321 m/s. Generally speaking, the numerical simulation catch up well with experimental data and has good prediction of bubble size distributions for all cases except flow condition of $\langle j_f \rangle$ =0.986 m/s and $\langle j_g \rangle$ =0.321 m/s. For this flow condition of =0.986 m/s and =0.321 m/s, both two drag correlations show under-predicted Sauter mean bubble diameter at the core but reasonable prediction in the vicinity of the wall area (Figure 5h). One of the possible reasons could be that Yao and Morel (2004) model which adopted in current study ignored wake entrainment phenomenon. Moreover, cap bubbles flow condition and wake entrainment phenomenon enlarge the range of Sauter mean bubble diameter distributions. Therefore, the numerical simulation for these flow conditions might be difficult to catch up with experimental results by ABND model which only presenting average Sauter bubble diameter by one group of population balance equation (Cheung et al. 2007 a and b).

4.3 Time-averaged gas velocity

The measured and predicted radial profiles of the air velocity at the measuring location of Z/D=53.5 close to the outlet of the pipe are shown in Figure 6. As depicted, in compared with Ishii and Zuber's model (1979), the Simonnet et al. (2007) drag coefficient correlation gives better predictions of the gas velocity profiles in most of flow cases. As proposed by Simonnet et al. (2007), the drag coefficient has the tendency to increase with gas void fraction when gas void fraction is less than 15%. However, when gas void fraction is beyond this critical value of 15%, the aspiration in the bubbles wakes becomes dominant and results in a decreased drag coefficient with the local void fraction. In order to further illustrate the improvement of Simonnet et al. (2007) drag coefficient. Conception of error percentage of gas velocity is introduced as:

$$error = \frac{\left| u_g - u_g^{'} \right|}{u_g^{'}} \times 100\% \tag{22}$$

where u_g and u_g' are predicted and experimental gas velocity, respectively. The error percentage presents the accuracy of simulation results comparing with experimental data. In Figure 7, the error percentage of time-averaged gas velocity are plotted against the axial position of Z/D=6.0 and 53.5. The solid and dash dot line indicate the simulation of Simonnet et al. (2007) and Ishii and Zuber (1979), respectively. As shown, drag coefficient correlation of Simonnet et al. (2007) can give considerably better predictions in time averaged gas velocity for most of flow conditions since it shows low error percentage values for Simonnet et al. (2007) model along axial position for most of cases.

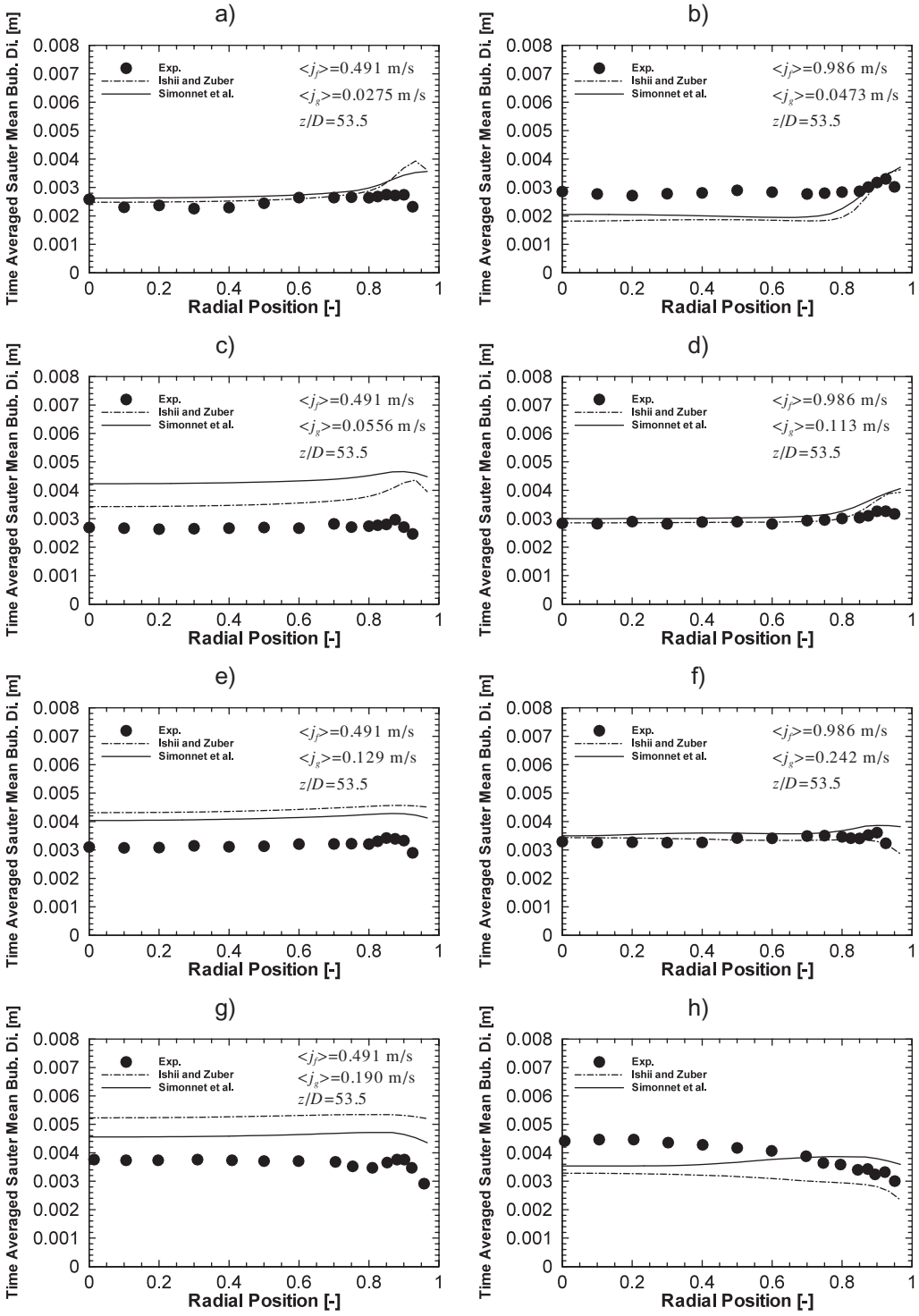

Figure 5. Predicted Sauter mean bubble diameter distributions and experiment data of Hibiki et al. (2001) at D/Z = 53.5.

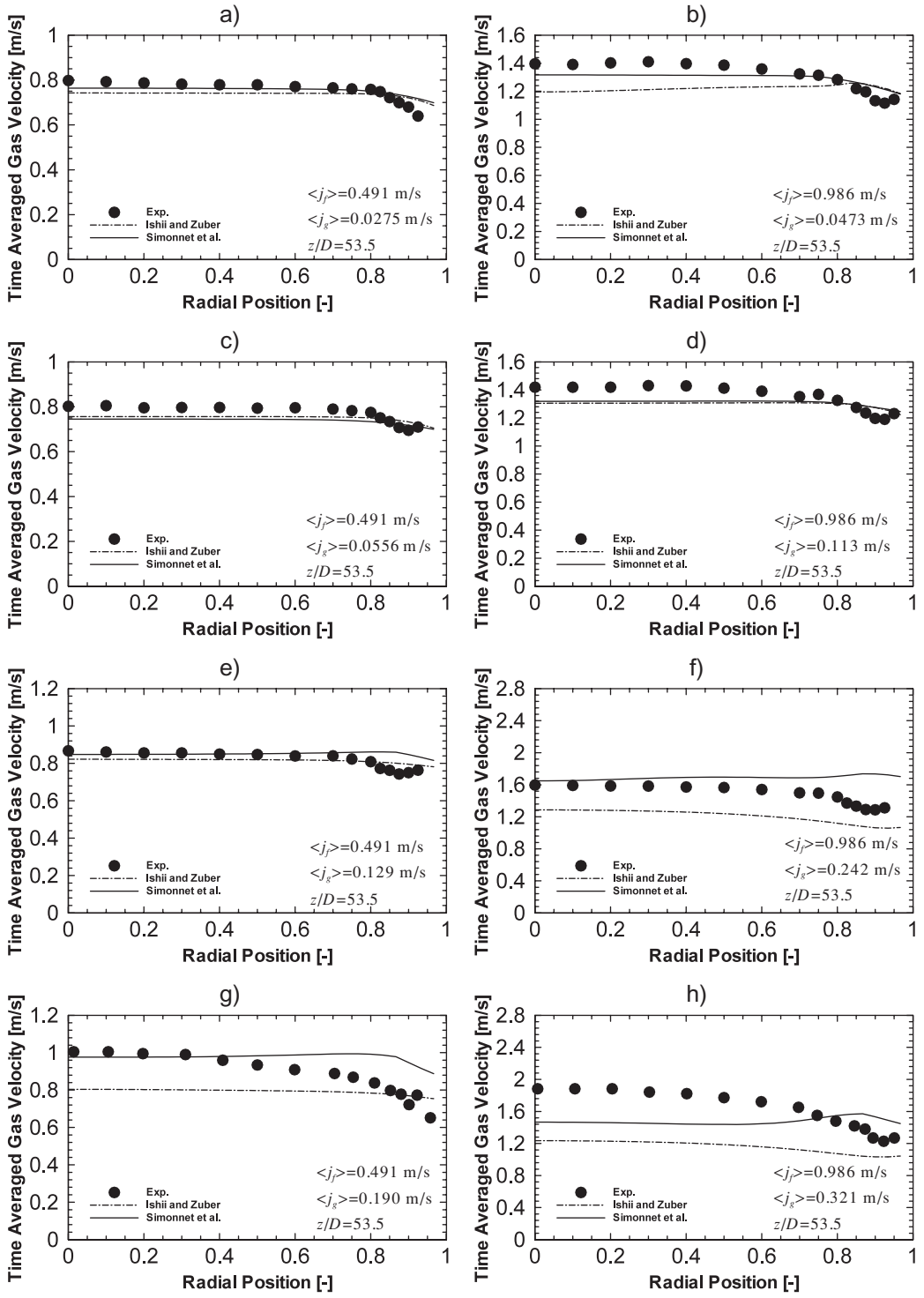

Figure 6. Predicted radial gas velocity profiles and experiment data of Hibiki et al. (2001) D/Z = 53.5.

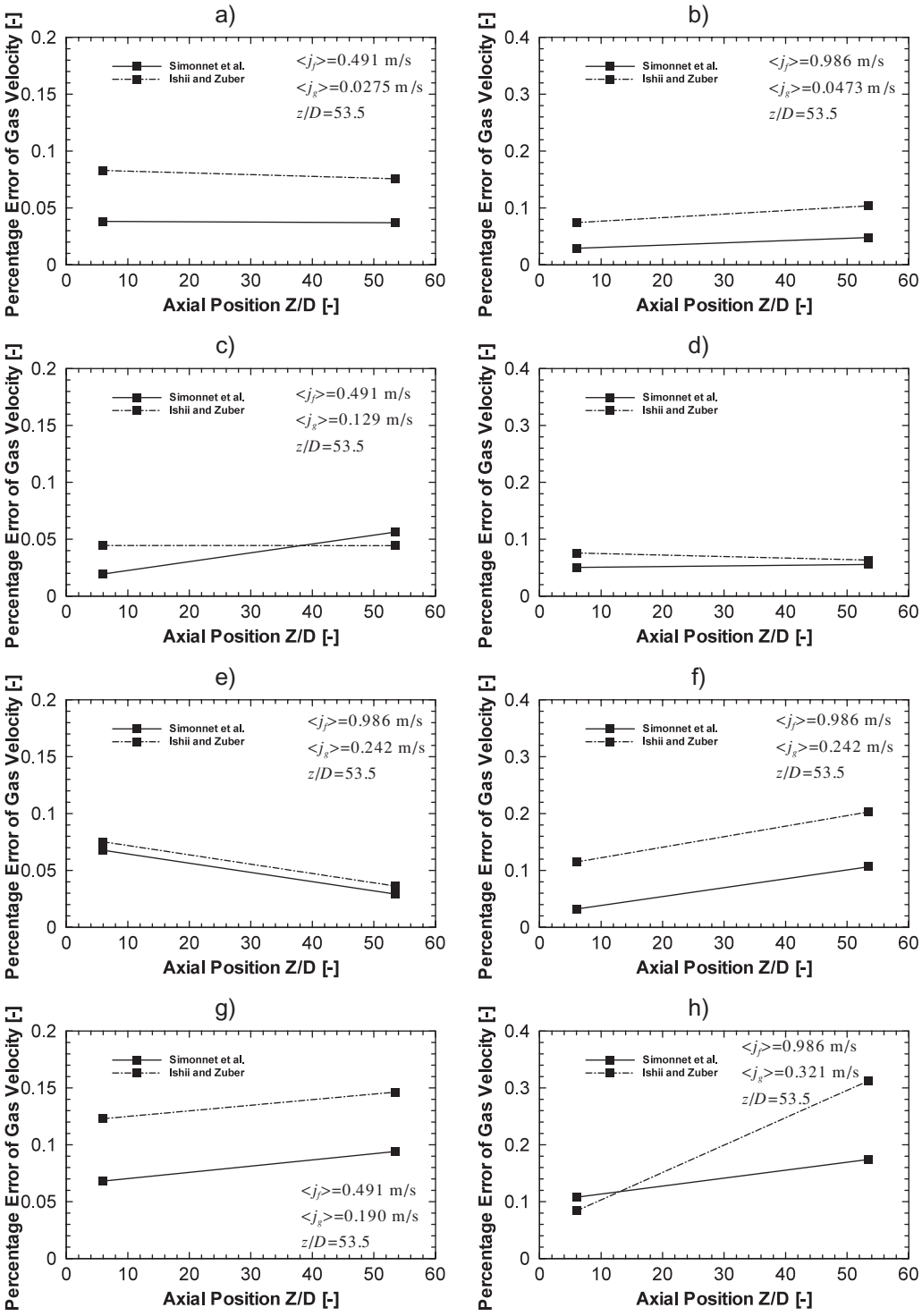

Figure 7. Error percentages of time averaged gas velocity comparing with experimental data of Hibiki et al. (2001).

5. CONCLUSIONS

An averaged one-group population balance approach, the average bubble number density (ABND) transport equation, coupled with the Eulerian-Eulerian two-fluid model is presented in this paper to handle the gas-liquid bubbly flows under isothermal conditions, particularly under bubbly-to-slug transition regime. Based on ABND model, drag mechanisms developed by Simonnet et al. (2007) and Ishii and Zuber (1979) respectively are compared against experimental data measured by Hibiki et al. (2001) under various flow conditions. Local radial distributions of three primitive variables: void fraction, Sauter mean bubble diameter and gas velocity, are compared. In general, both of the drag coefficient correlations predictions yield fair agreement with experimental results. With additional consideration for closely packed bubbles, the latest coefficient model by Simonnet et al. (2007) in terms of local void fractions shows considerably better performance in capturing the influence from neighbouring bubbles.

Among the eight cases, notable discrepancies are found between the numerical and experimental results in flow condition with higher void fraction and higher liquid/gas velocity (i.e. $\langle j_f \rangle$=0.986 m/s and $\langle j_g \rangle$=0.321 m/s). The reason of these discrepancies could be due to the usage of one group equation to present averaged Sauter mean bubble diameter in ABND model since bubble diameter has wider range under these flow conditions than others. Moreover, another possible reason of numerical inaccuracy may be ignoring wake entrainment phenomenon in Yao and Morel (2004) model for ABND equations source and sink terms. Finally, Tomiyama (1998) lift coefficient model only considered the behaviour of single distorted bubble under stagnant flow condition. The lift force in multi-bubble system is needed further developed.

ACKNOWLEDGMENTS

The financial support is provided by the Australian Research Council (ARC-Discovery DP0877734) is gratefully acknowledged and the first author is also supported by RMIT University through International Post Graduate Research Scholarship (IPRS).

REFERENCES

Antal S.P., Lahey Jr., R.T., Flaherty J.E., (1991). Analysis of phase distribution in fully developed laminar bubbly two-phase flow. *Int. J. Multiphase Flow*, 17, 635

Bannari R., Kerdouss F., Selma B., Bannari A., Proulx P. (2008). Three dimensional mathematical modelling of dispersed two phase flow using class method of population balance in bubble columns. *Comput. Chem. Eng*., 32, 3224.

Behzadi A., Issa R. I., Rusche H. (2004). Modelling of dispersed bubble and droplet flow at high phase fractions, *Chem. Eng. Sci*., 59, 759.

Bertola F., Baldi G., Marchisio D., Vanni M. (2004). Momentum transfer in a swarm of bubbles: estimates from fluid-dynamic simulations, *Chem. Eng. Sci.,* 59, 5209.

Bhaga D, Weber M.E. (1981). Bubble in viscous liquids: shapes, wakes and velocities, *J. Fluid Mech*., 105, 61.

Bhole M. R., Joshi J. B., Ramkrishna D. (2008). CFD simulation of bubble columns incorporating population balance modelling. C*hem. Eng. Sci*., 63, 2267.

Burns A.D., Frank T., Hamill I., Shi, J. (2004). The Farve averaged drag model for turbulent dispersion in Eulerian Multi-phase flows, in: *Proceeding of the Fifth International Conference on Multiphase flow*, Yokohama, Japan.

Chen p., Sanyal J., Dudukovic M. P. (2005). Numerical simulation of bubble columns flows: effect of different breakup and coalescence closures. *Chem. Eng. Sci*., 60, 1085.

Cheung S.C.P., Yeoh G.H., Tu J.Y. (2007) a. On the modelling of population balance in isothermal vertical bubbly flows – average bubble number density approach. *Chem. Eng. Process*., 46, 742.

Cheung S.C.P., Yeoh G.H., Tu J.Y. (2007) b. On the numerical study of isothermal vertical bubbly flow using two population balance approaches. *Chem. Eng. Sci*., 62, 4659.

Churchill S. W. (1989). A theoretical structure and correlating equation for the motion of singe bubbles. *Chem. Eng. Pro*., 26, 269.

Clift R., Grace J. R., Weber M. E. (1978). *Bubble, Drops, and Particles*. Academic Press, New York.

Davidson J. F., Harrison D. (1966). The behaviour of a continuously bubbling fluidised bed. *Chem. Eng. Sci*., 21, 731.

Drew D.A., Lahey Jr., R.T. (1979). Application of general constitutive principles to the derivation of multidimensional two-phase flow equation. *Int. J. Multiphase Flow*, 5, 243.

Frank T., Shi J., Burns F A.D. (2004). Validation of Eulerian multiphase flow models for nuclear safety application, in: *Proceedings of the third international symposium on two phase modelling and experimentation*, Pisa, Italy

Grace, J. R. (1973). Shapes and velocities of bubbles rising in infinite liquids. *Trans. Chem. Eng*., 51, 116

Grienberger J., Honfmann H. (1992). Investigations and modelling of bubble columns. *Chem. Eng. Sci*., 47, 2215.

Hibiki T., Ishii M. (2000). One-group interfacial area transport of bubbly flows in vertical round tubes. *Int. J. Heat Mass Trans*., 43, 2711.

Hibiki T., Ishii M. (2002). Development of one-group interfacial area transport equation in bubbly flow systems. *Int. J. Heat Mass Trans*., 45, 2351.

Hibiki T., Ishii M., Xiao Z., (2001). Axial interfacial area transport of vertical bubble flows. *Int. J. Heat Mass Trans*., 44, 1869.

Hibiki T., Ishii M. (2007). Lift force in bubbly flow systems. *Chem. Eng. Sci*., 62, 6457.

Ho M.K., Yeoh G.H., (2005). Phenomenological investigation of gas-liquid flows. *Trans. American Nucl. Soci*., 93, 408.

Ishii M., Zuber N. (1979). Drag coefficient and relative velocity in bubbly, droplet or particulate flows. *A.I.Ch.E. Journal*, 5, 843.

Jamialahmadi M., Branch C., Muller-Steinhagen H., (1994). Terminal bubble rise velocity in liquids. *Trans. Ins. Chem. Eng*., 72(A)

Kendoush A.A. (2001). Hydrodynamic model for bubbles in a swarm. *Chem. Eng. Sci*., 56, 235.

Kendoush A.A., Mohammed T. J., Abid B. A., Hameed M. S. (2004). Experimental investigation of the hydrodynamic interaction in bubbly two-phase flow. *Chem. Eng. and Processing*. 43, 23.

Lahey Jr., R.T., Sim S., Drew D.A., (1979). An evaluation of interfacial drag models for bubbly two-phase flow. In: Chen, J.C., BankoE, S.G., (Eds.), *ASME 18th National Heat Transfer Conference*, New York, USA, 11.

Liu Y., Hibiki T., Ishii M., Kelly J. M. (2008). Drag coefficient in one-dimensional two-group two-fluid model. *Int. J. Heat Fluid Flow,* 29, 1402.

Mabrouk R., Chaouki J., Guy C. (2007). Effective drag coefficient investigation in the acceleration zone of an upward gas-solid flow. *Chem. Eng. Sci*., 62, 317.

Magnaudet J., Eames I. (2000). The motion of high-Reynolds-Number Bubbles in Inhomogeneous flows. *Annu. Rev. Fluid Mech*., 32, 659.

Mei R, Klausner JF, Lawrence CJ. (1994). A note on the history force on a spherical bubble at finite Reynolds number. *Phys. Fluids* 6, 418.

Moore DW. (1965). The velocity of rise of distorted gas bubbles in a liquid of small viscosity. *J. Fluid Mech.* 23, 749.

Olmos E., Gentric C., Vial Ch., Wild G., Midoux N. (2001). Numerical simulation of multiphase flow in bubble column. Influence of bubble coalescence and break-up. *Chem. Eng. Sci*., 56, 6359.

Politano M. S., Carrica P.M., Converti J. (2003). A model for turbulent polysidperse two phase flow in vertical channels. *Int. J. of Multiphase Flow*, 29, 1153

Rusche H., Issa R. I. (2000). The effect of voidage on the drag force on particles, droplets and bubbles in dispersed two-phase flow. In *Japanese European Two-Phase Flow Meeting*, Tshkuba, Japan.

Sato Y., Sadatomi M., Sekoguchi K., (1981). Momentum and heat transfer in two-phase bubbly flow – I. *Int. J. of Multiphase Flow*, 7, 167.

Simonnet M., Gentric C., Olmos E., Midoux N. (2007). Experimental determination of the drag coefficient in a swarm of bubbles. *Chem. Eng. Sci*., 62, 858.

Simonnet M., Gentric C., Olmos E., Midoux N. (2008). CFD simulation of the flow field in a bubble column reactor: Importance of thedrag force formulation to describe regime transitions. *Chem. Eng. and Processing*, 47, 1726.

Tabib M.V., Roy S. A., Joshi J. B. (2008). CFD simulation of bubble column-An analysis of interphase forces and turbulence models. *Chem. Eng. J*., 139, 589.

Taylor TD, Acrivos A. (1964). On the deformation and drag of a falling viscous drop at low Reynolds number. *J. Fluid Mech.* 18, 466.

Tomiyama A. (1998). Struggle with computational bubble dynamics. *Proceedings of the Third International Conference on Multiphase Flow*. Lyon, France.

Tomiyama A. (2004). Drag, lift and virtual mass forces acting on a single bubble. *Proceedings of the Third International Symposium on Two-phase Flow Modelling and Experimentation*, Pisa, Italy, Paper No. il01.

Wallis G.B. (1969). *One-Dimensional Two-Phase Flow*. McGraw Hill, New York.

Wu Q., Kim S., Ishii M., Beus S.G., (1998). One-group interfacial area transport in vertical bubbly flow. *Int. J. Heat Mass Trans*., 41, 1103.

Yao W., Morel C., (2004). Volumetric interfacial area prediction in upwards bubbly two-phase flow. *Int. J. Heat Mass Trans*., 47, 307.

Zhang L., Yang C., Mao Z. X. (2008). Unsteady motion of a single bubble in highly viscous liquid and empirical correlation of drag coefficient. *Chem. Eng. Sci*., 63, 2099.